SafeNet

Safeguarding Biodiversity and Carbon-rich Forest Networks in Europe

Mapping European forest carbon

28/02/2026 Version 2

Amy C. Bennett
a.c.bennett@leeds.ac.uk

Funded by the European Union

Funded by the European Union under the Horizon Europe Programme, Grant Agreement No. 101181981 (SafeNet). Views and opinions expressed are, however, those of the author(s) only and do not necessarily reflect those of the European Union or European Research Executive Agency (REA). Neither the European Union nor the granting authority can be held responsible for them.

Document information

Grant agreement	101181981
Project Acronym	SafeNet
Project Title	Safeguarding Biodiversity and Carbon-rich Forest Networks in Europe
Deliverable number	2.2, D5
Work Package Number (Task Number)	WP2 (T2.2)
Deliverable Name	Map of current forest carbon distribution
Lead Partner	University of Leeds, Leeds, UK
Author(s)	Amy C. Bennett Catherine E. Scott Dominick V. Spracklen
Due Date	28.02.26
Submission Date	28.02.26
Dissemination Level	PU
Type of Deliverable	R

Version	Date	Institution	People	Summary of Changes
1.0	30/01/2026	University of Leeds	Amy Bennett	Draft document.
2.0	28/02/2026	University of Leeds	Amy Bennett	Revision based on review by Bill Kunin (University of Leeds), Mikko Peltoniemi (LUKE), Alba Viana Soto (TUM).

Contents

1. Introduction

Forest carbon stocks vary widely across Europe due to differences in climate, species composition, soil conditions and land-use history. We combine products based on forest inventory data, remote-sensing, soil and climate datasets to generate a comprehensive map of current forest carbon distribution including above- and belowground components. Deliverable 2.2 (also D5, T2.2) provides an integrated forest carbon density map for 2020, at 100 x 100 m resolution, and is designed to support subsequent tasks within SafeNet. It is available on Zenodo.

Table 1 | List of abbreviations used in this document.

Abbreviation	Meaning
AGB	Aboveground biomass
AGC	Aboveground (biomass) carbon
BD	Bulk density
BGB	Belowground biomass
BGC	Belowground (biomass) carbon
C	Carbon
CF	Coarse fragments (soil characteristic)
MAT	Mean annual temperature
NFI	National Forest Inventory
SOC	Soil organic carbon

Report citation[1]: Bennett, A.C., Scott, C.E., and Spracklen, D.V. (2026). SafeNet D2.2 Mapping European forest carbon. Zenodo. https://doi.org/10.5281/zenodo.18818508

Dataset: Bennett, A.C., Scott, C.E., and Spracklen, D.V. (2026). SafeNet D2.2 European forest carbon maps. [Data set]. Zenodo. https://doi.org/10.5281/zenodo.18412966

[1] Bennett, A. C., Scott, C. E., & Spracklen, D. V. (2026). SafeNet D2.2 Maps of European forest carbon [Data set]. Zenodo. https://doi.org/10.5281/zenodo.18412966.

2. Methods

The methods described in this report detail how we produced maps of forest carbon density across Europe for the year 2020. Our approach broadly follows the process used by Spawn et al., (2020)[2] who integrated multiple datasets of aboveground biomass, forest type and carbon fraction to estimate aboveground biomass carbon and model belowground biomass for 2010 at 300 m resolution. We applied the same conceptual approach but used different, more recent input datasets and generated outputs at a higher (100 m) resolution.

We generated a spatially explicit map of forest carbon density across Europe by combining datasets for aboveground biomass carbon (AGC), belowground biomass carbon (BGC) and soil organic carbon (SOC), which were summed to calculate total forest carbon (C).

$$C = AGC + BGC + SOC$$

Our workflow (Figure 1) included climate and forest type classification, carbon-fraction assignment, biomass-to-carbon conversions, estimation of belowground biomass carbon using published regression models, and calculation of soil carbon stocks from gridded soil properties. All spatial layers were pre-processed to a common 100 m grid and restricted to the SafeNet project boundary. Data gaps were filled using an hierarchical approach, initial values were populated via a multi-pass focal mean filter (3x3,5x5,7x7 windows). Once <3% of values were missing, remaining pixels were assigned the median raster value to ensure a continuous carbon stock estimate. For the forest origin layer, remaining gaps were assigned the 'planted' category, although 'natural' is the dominant forest type, this provides a more conservative estimate of BGC. As the PathFinder[3] products (including the European forest biomass map) do not cover Russia, our analysis was limited to pixels within the PathFinder spatial extent. This ensures consistent spatial coverage and comparability across all carbon pools. Throughout this report, 'forest pixels of the project area' refers to these 100 x 100 m forest cells where all required data were available.

To evaluate our outputs we compared our estimates of AGC, BGC and SOC to published products to provide a validation of our carbon layers. We extracted values at 1000 randomly

[2] Spawn, S. A., Sullivan, C. C., Lark, T. J., & Gibbs, H. K. (2020). Harmonized global maps of above and belowground biomass carbon density in the year 2010. Scientific Data, 7(1), 112. https://doi.org/10.1038/s41597-020-0444-4

[3] Miettinen, J., Breidenbach, J., Adame, P., Adolt, R., Alberdi, I., Antropov, O., Astrup, R., Berger, A., Chirici, G., Corona, P., D'Amico, G., Fejfar, J., Fischer, C., Gohon, F., Gschwantner, T., Hertzler, J., Koma, Z., Korhonen, K. T., Krajnc, L., … Wurpillot, S. (2025). PathFinder's High-Resolution Pan-European Forest Structure Maps: An Integration of Earth Observation and National Forest Inventory Data.

generated points, compared pixel-level values across datasets and produced a spatial difference map to highlight areas of agreement and divergence.

The outputs are four rasters (AGC, BGC, SOC and total C), at 100 m x 100 m resolution, available online (Bennett et al., 2026; Zenodo)[4]. These Europe-wide carbon maps are designed to support subsequent analyses within SafeNet and to provide a reproducible, transparent baseline for forest carbon assessments. All geospatial and statistical analyses were conducted in R (version 4.5.2) and Google Earth Engine.

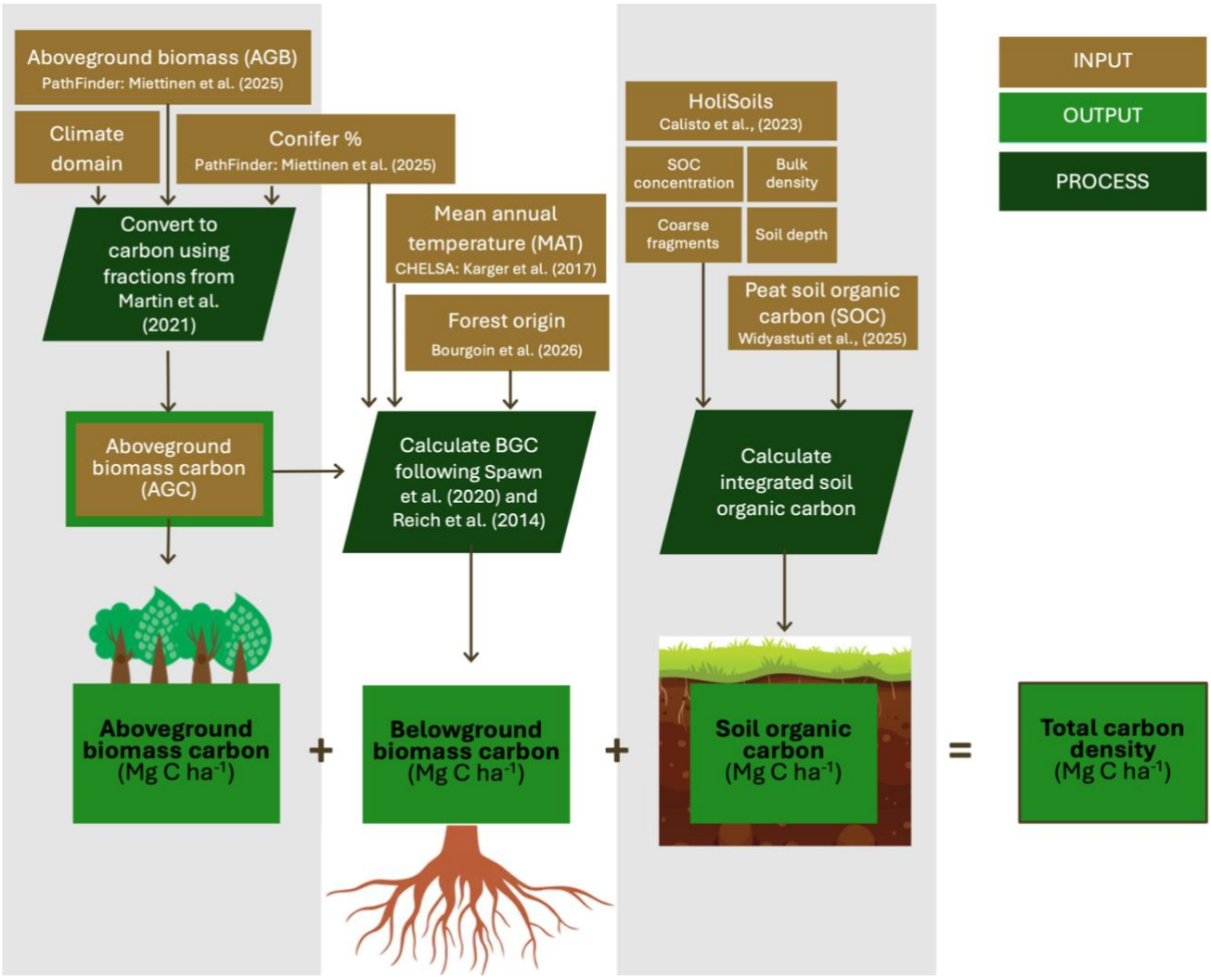

Figure 1 | Methods flow chart.

[4] Bennett, A. C., Scott, C. E., & Spracklen, D. V. (2026). SafeNet D2.2 Maps of European forest carbon [Data set]. Zenodo. https://doi.org/10.5281/zenodo.18412966.

2.1 Aboveground biomass carbon

We follow the process detailed in Spawn et al., (2020)[2] to convert AGB to AGC. Aboveground biomass inputs were from the PathFinder[3] European forest biomass dataset, which harmonises National Forest Inventory (NFI) plot measurements with Sentinel-2 multispectral imaging and tree cover density and forest type from the Copernicus Land Monitoring Service[5]. PathFinder is available at 10 x 10 m resolution, maintaining the detail from remote sensing observations and the consistency of ground-based measurements. Other remote-sensing biomass products lack this cross-country harmonisation. PathFinder also provides data on the proportion of biomass from conifers which is information that we use when estimating carbon from biomass.

We converted aboveground biomass (PathFinder[3]) to carbon using climate- and phylogeny-specific fractions from Martin et al., (2018)[6], listed in Table 2. We first aggregated the 10 x 10 m dataset to 100 x 100 m pixels, a compromise between the detail from the high resolution of PathFinder and coarser resolutions of soil and climate predictors, and considering computational requirements. We aggregated using a mean function, where NA values in the AGB layer were reclassified to zero prior to upscaling to ensure our carbon density accounts for forest edges and gaps. To assign the appropriate fraction to each pixel we classified every cell as Boreal, Temperate or Subtropical/Mediterranean using the Koppen-Geiger climate classifications[7] (1991-2020, Figure 3, Figure 4). We then used the PathFinder[3] conifer proportion of aboveground biomass product (mean=45 %, Figure 5) to weight the conversion factor per pixel. Across the project area, forests are mainly Temperate (64%), followed by Boreal (21%), then Subtropical/Mediterranean (15%). All input layers were resampled and aligned to the PathFinder 100 m grid to ensure consistent pixel-level integration. We combined climate domain and conifer-proportion to calculate the carbon fraction (Table 2) for each pixel and convert aboveground biomass to aboveground carbon (AGC, Mg C ha^{-1}) (Figure 6). The output is a 100 x 100 m AGC map.

[5] European Environment Agency (EEA). (2021). High Resolution Layer: Forest Type and Tree Cover Density (reference year 2018). Copernicus Land Monitoring Service (CLMS). Available at: https://land.copernicus.eu/en/products/high-resolution-layers/forests
[6] Martin, A. R., Doraisami, M., & Thomas, S. C. (2018). Global patterns in wood carbon concentration across the world's trees and forests. Nature Geoscience, 11(12), 915–920. https://doi.org/10.1038/s41561-018-0246-x
[7] Beck, H. E., McVicar, T. R., Vergopolan, N., Berg, A., Lutsko, N. J., Dufour, A., Zeng, Z., Jiang, X., van Dijk, A. I. J. M., & Miralles, D. G. (2023). High-resolution (1 km) Köppen-Geiger maps for 1901–2099 based on constrained CMIP6 projections. Scientific Data, 10(1), 724. https://doi.org/10.1038/s41597-023-02549-6

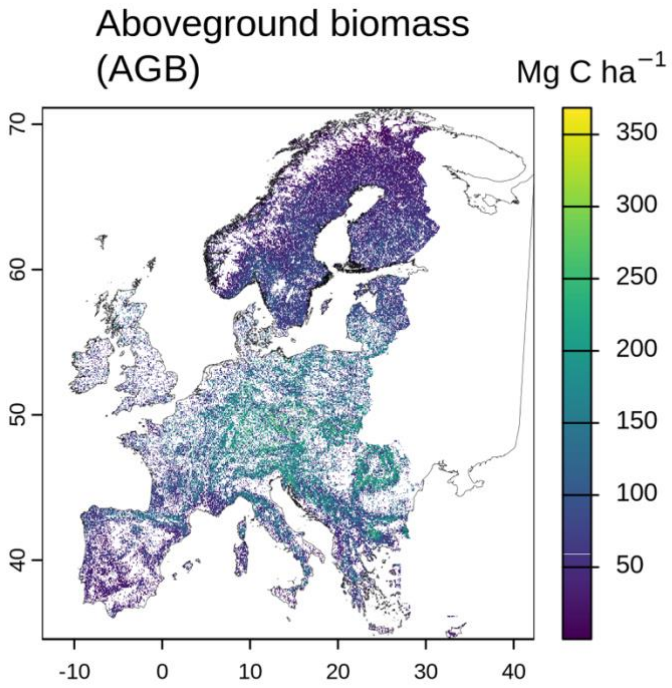

Figure 2 | Aboveground biomass input (Miettinen et al., (2025)[3]).

Table 2 | Carbon fraction of aboveground biomass[6].

Climate zone	Phylogeny	Mean
Subtropical / Mediterranean	Angiosperm	0.465
	Gymnosperm	0.484
Temperate	Angiosperm	0.472
	Gymnosperm	0.489
Boreal	Angiosperm	0.488
	Gymnosperm	0.476

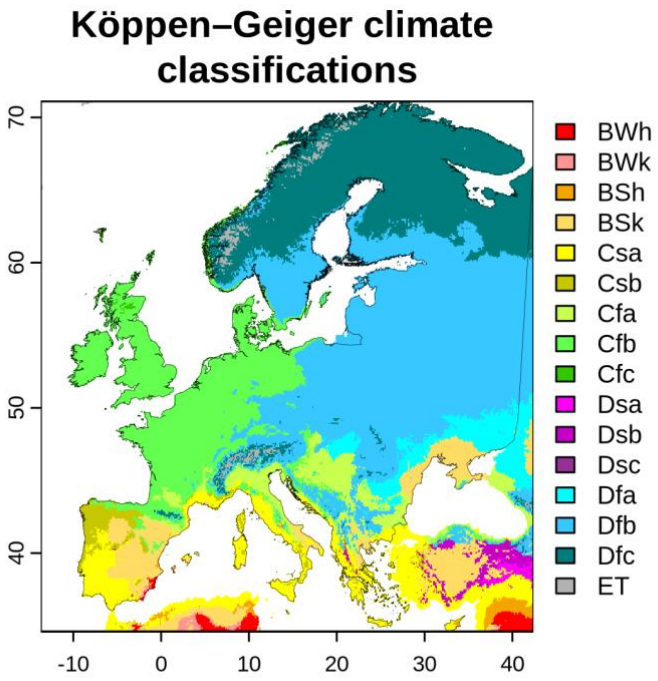

Figure 3 | Koppen-Geiger climate classifications (1991-2020)[7] used to map climate domains (Figure 4).

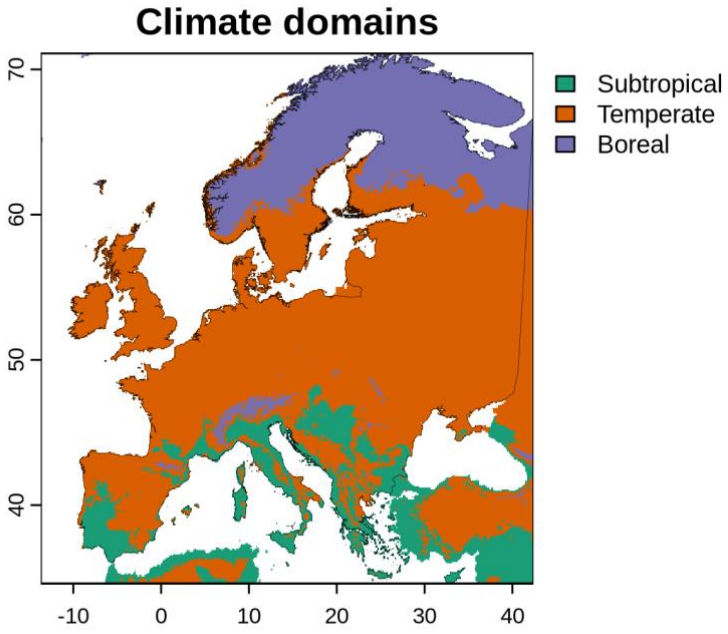

Figure 4 | Climate domains used to convert aboveground biomass to aboveground carbon.

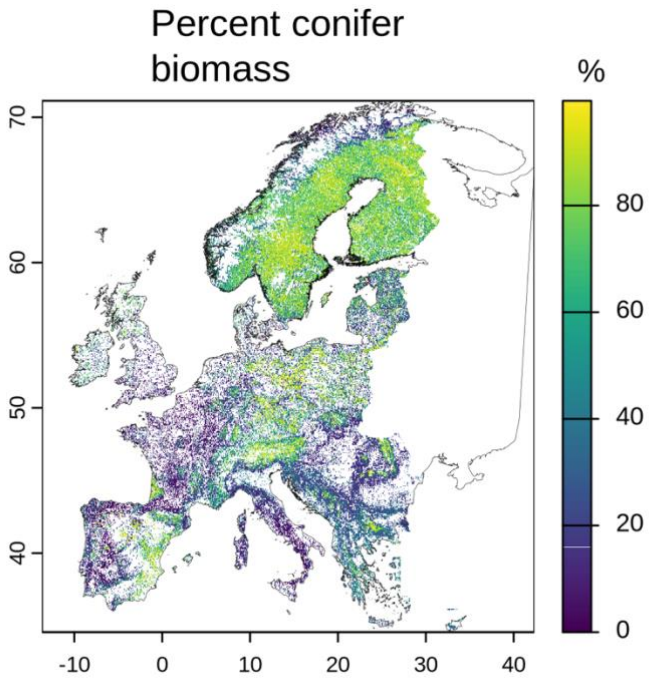

Figure 5 | Percentage of aboveground biomass from conifers[3].

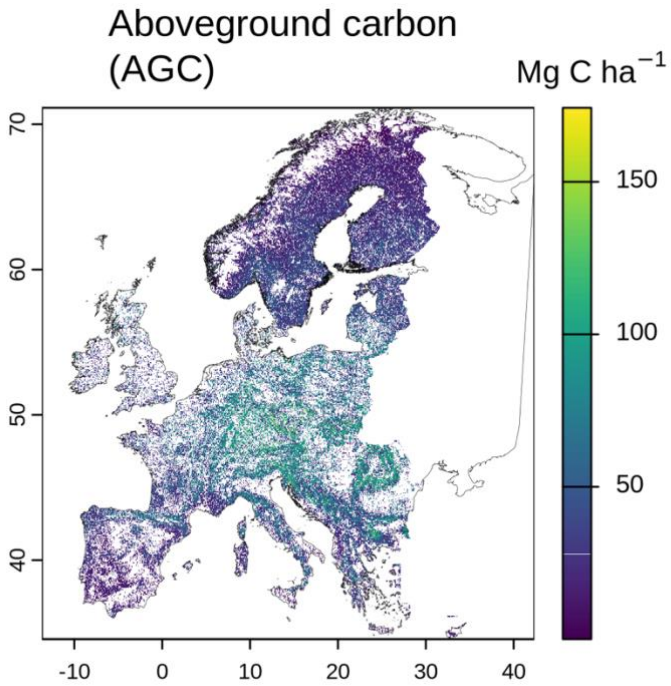

Figure 6 | Aboveground biomass carbon map.

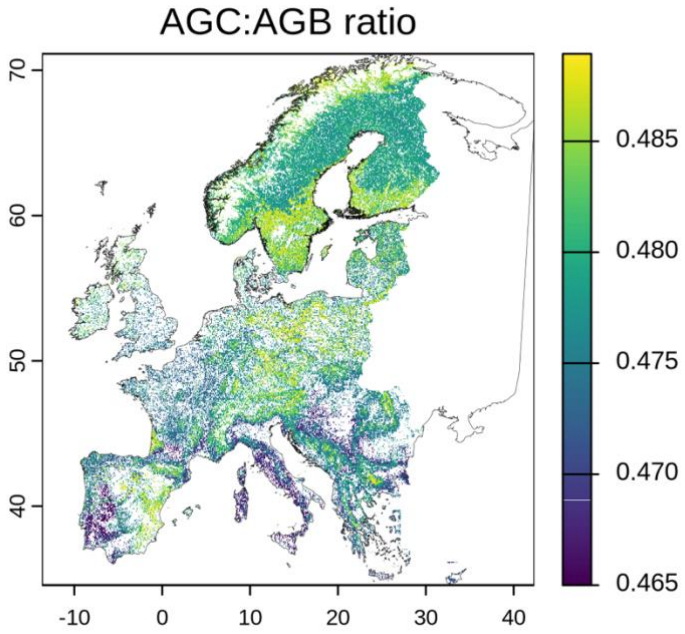

Figure 7 | Ratio between AGC (calculated in this work) and input AGB (PathFinder[3]).

We see disproportionately higher carbon fractions of AGB in cool, gymnosperm-dominated northern forests and lower ratios in warm, angiosperm-dominated regions, and a mean carbon fraction of aboveground biomass of 0.478 (Figure 7).

Validation of AGC map

Overall, our AGC map is consistent with existing AGC maps when inspecting visually, including aboveground carbon stock in 2010 (10 km x 10 km)[8], reproducing major regional patterns such as high carbon densities in Central European mixed forests and lower values in boreal conifer stands.

To evaluate our AGC estimates we compared our AGC values at 1,000 randomly generated points to the 2010 aboveground carbon global map produced by Spawn et al., (2020). Our AGC corresponded with theirs ($r=0.5$, $p<0.001$). We find an average of 1.2 Mg C ha^{-1} more carbon per pixel, which is consistent with increased biomass in Europe through forest growth

[8] Gallaun, H., Zanchi, G., Nabuurs, G.-J., Hengeveld, G., Schardt, M., & Verkerk, P. J. (2010). EU-wide maps of growing stock and above-ground biomass in forests based on remote sensing and field measurements. Forest Ecology and Management, 260(3), 252–261. https://doi.org/10.1016/j.foreco.2009.10.011

and succession over the last decade. The Root Mean Square Error (RMSE) of 21 indicates variability at the pixel level.

We produced a difference map between the products by subtracting Spawn et al., (2020) from our map (Figure 8), to identify areas where there may be differences in aboveground carbon. Spatial divergence was most apparent in central Europe where we observe both higher and lower carbon compared to the 2010 dataset. The divergence may reflect changes in forest carbon over time via succession, harvest, disturbance or degradation, or differences in sensor resolution. Whilst our map captures the expected regional trends, a high RMSE evidences the challenges of comparisons across temporal and spatial resolutions and sensing technologies, hence the extent to which we can validate our output is limited.

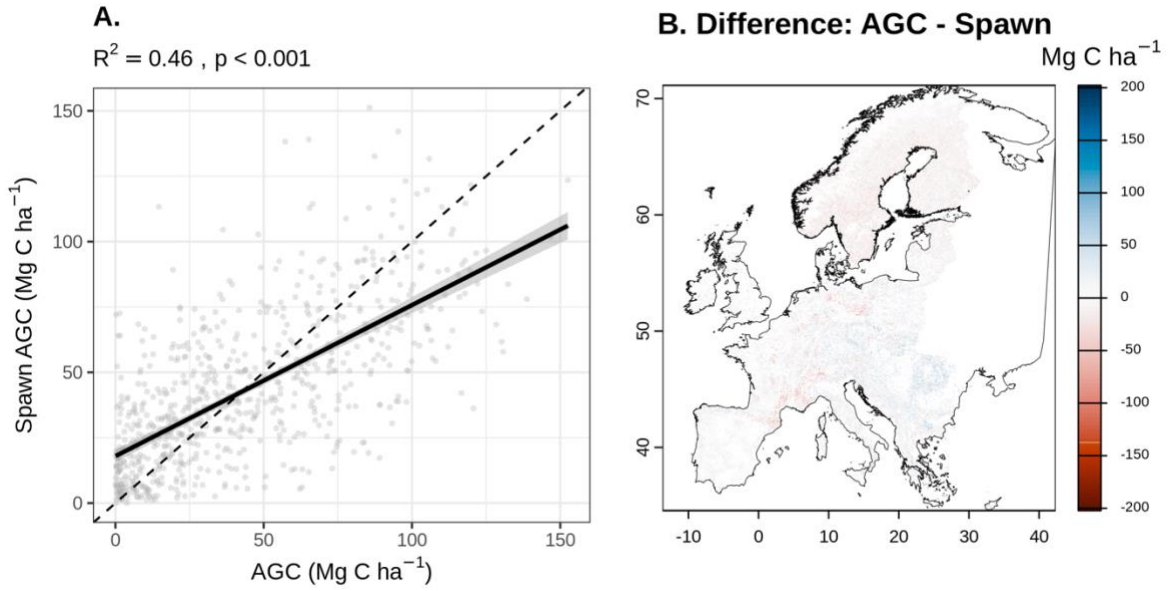

Figure 8 | Validation of AGC (calculated in this work) and AGC (Spawn et al., (2020)[2]). Carbon estimates extracted at 1,000 random points (A), and difference map of all forest pixels (B).

2.2 Belowground biomass carbon

Belowground carbon was modelled from our 100 m AGC product to ensure spatial and internal consistency across all carbon pools. By modelling BGC directly from AGC we maintain the 100 m resolution of the PathFinder dataset and ensure that root-to-shoot ratios are calculated using the same pixel-level canopy information.

Following the methods of Spawn et al., (2020)[2], we spatially applied the regression models developed by Reich et al., (2014, see Table S6)[9]:

$$\log10(\mathrm{BGC}) = \alpha + \beta \mathrm{MAT}_c + \gamma \mathrm{S}_c + \delta(\mathrm{MAT}_c \cdot \mathrm{S}_c)$$

Where:

$\mathrm{MAT}_c = \mathrm{MAT} - 9.1374$ (°C) and

$\mathrm{S}_c = \log10(\mathrm{AGC}) - 1.88807$

This model predicts root biomass based on AGC, mean annual temperature (MAT), phylogeny (conifer vs. broadleaf), and regenerative origin (natural vs. planted). Parameter values were taken from Reich et al., (2014)[9], stratified by forest domain, weighted by regenerative origin, and applied per pixel.

Table 3 | Coefficients for converting AGC to BGC[9].

Phylogeny	Regeneration	α	β	γ	δ
Gymnosperm	Planted	-0.18088	-0.003032	0.7940911	0.0020443
	Natural	-0.17907	-0.003587	0.8155491	0.0036998
Angiosperm	Planted	-0.16361	-0.004455	0.7623551	0.0071044
	Natural	-0.16239	-0.0029516	0.810802	0.0087599

While AGC is the primary predictor of root biomass carbon (BGC), the interaction term (δ) accounts for the effect of temperature. This interaction is stronger for angiosperms than gymnosperms, indicating that higher temperatures amplify biomass partitioning to roots more significantly in broadleaf species than in conifers.

We acknowledge the ongoing debate regarding 'optimal partitioning theory' (Robinson, 2022), which suggests root-to-shoot ratios are dynamic and driven by local resource availability rather than global patterns. Additionally, a compilation of global field-data (Huang et al., (2021))[10] indicated that remotely sensing-products often have lower belowground

[9] Reich, P. B., Luo, Y., Bradford, J. B., Poorter, H., Perry, C. H., & Oleksyn, J. (2014). Temperature drives global patterns in forest biomass distribution in leaves, stems, and roots. *Proceedings of the National Academy of Sciences*, *111*(38), 13721–13726. https://doi.org/10.1073/pnas.1216053111

[10] Huang, Y., Ciais, P., Santoro, M., Makowski, D., Chave, J., Schepaschenko, D., Abramoff, R. Z., Goll, D. S., Yang, H., Chen, Y., Wei, W., & Piao, S. (2021). A global map of root biomass across the world's forests. *Earth System Science Data*, *13*(9), 4263–4274. https://doi.org/10.5194/essd-13-4263-2021

biomass values than empirical models. The Reich et al., (2014) approach identified MAT as the primary global-scale driver of biomass partitioning at a continental scale, they used field-data and evaluated a suite-of potential predictors including water availability. Due to the logistical constraints of developing a high-resolution European-specific BGC model from primary data, we used the Reich model to estimate BGC from AGC at 100 m resolution. To benchmark our results against largescale data-driven findings, we validated our 100 m output against the 300 m resolution Spawn et al., (2020)[2] BGC dataset.

Spatial predictors were integrated at 100 m resolution from the following sources: mean annual temperature (CHELSA v2.1[11,12], Figure 9), proportion of biomass from conifers (PathFinder[7], Figure 5) and regenerative origin (natural or planted) from the global map of forest cover types for the year 2020 (GFT 2020[13], Figure 10). The GFT included primary, naturally regenerating and planted forest types. As we needed to distinguish between natural and planted forests, we used Google Earth Engine to combine the primary and naturally regenerating forest types into a single 'natural forest' category and exported as a raster to continue processing in R. Across the project area there were more natural (64 %) than planted (36 %) forest pixels.

[11] Brun, P., Zimmermann, N. E., Hari, C., Pellissier, L., & Karger, D. N. (2022). Global climate-related predictors at kilometer resolution for the past and future. Earth System Science Data, 14(12), 5573–5603. https://doi.org/10.5194/essd-14-5573-2022
[12] Karger, D. N., Conrad, O., Böhner, J., Kawohl, T., Kreft, H., Soria-Auza, R. W., Zimmermann, N. E., Linder, H. P., & Kessler, M. (2017). Climatologies at high resolution for the earth's land surface areas. Scientific Data, 4(1), 170122. https://doi.org/10.1038/sdata.2017.122
[13] Bourgoin, Clement; Ameztoy, Iban; Verhegghen, Astrid; Carboni, Silvia; Achard, Frederic; Colditz, Rene (2026): Global map of forest types 2020 - version 1. European Commission, Joint Research Centre (JRC) [Dataset] PID: http://data.europa.eu/89h/45182662-3015-4a25-8d1e-aa857d75235d

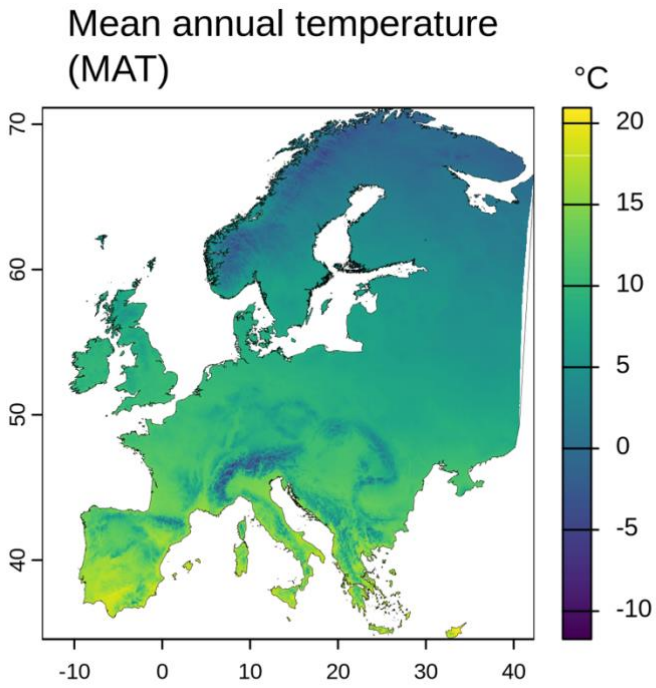

Figure 9 | Mean annual temperature (MAT) of project area (°C, 1981-2010)[9,10].

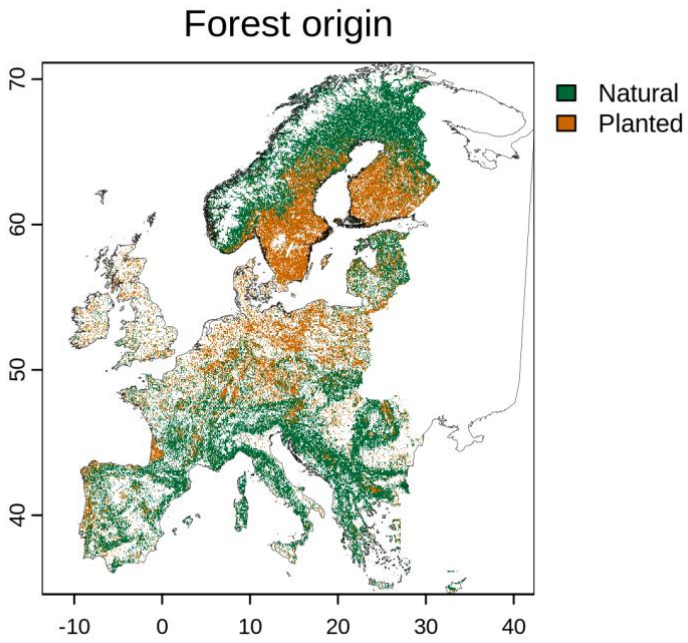

Figure 10 | Regenerative origin of forests in the project area.

Belowground biomass carbon estimates (BGC; Mg C ha^{-1}, Figure 11) reveal clear latitudinal gradients. Higher BGC occurs in central Europe, and lower BGC in northern boreal forests (due to thermal limitations and gymnosperm dominance) and xeric Mediterranean regions, where water deficits limit productivity and biomass stocks. Across the project area we find a mean BGC/AGC fraction of 0.26, so BGC is typically a quarter of AGC (Figure 20).

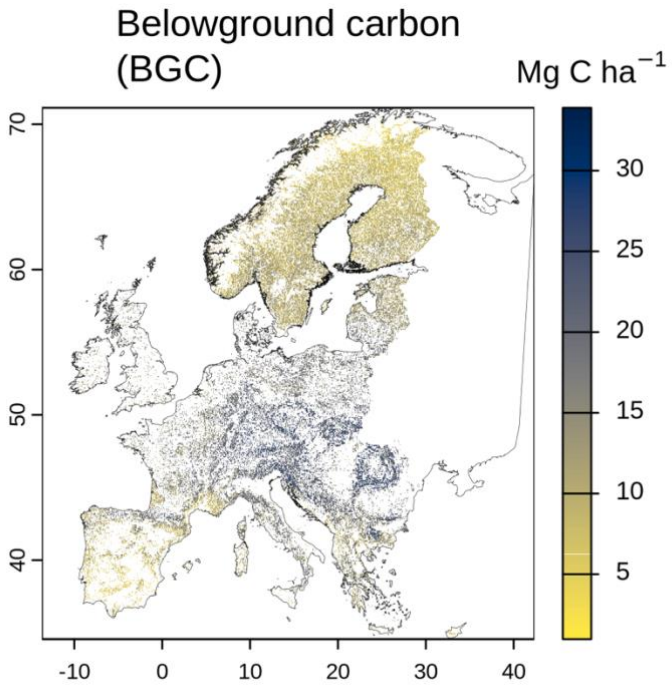

Figure 11 | Belowground biomass carbon (BGC) map.

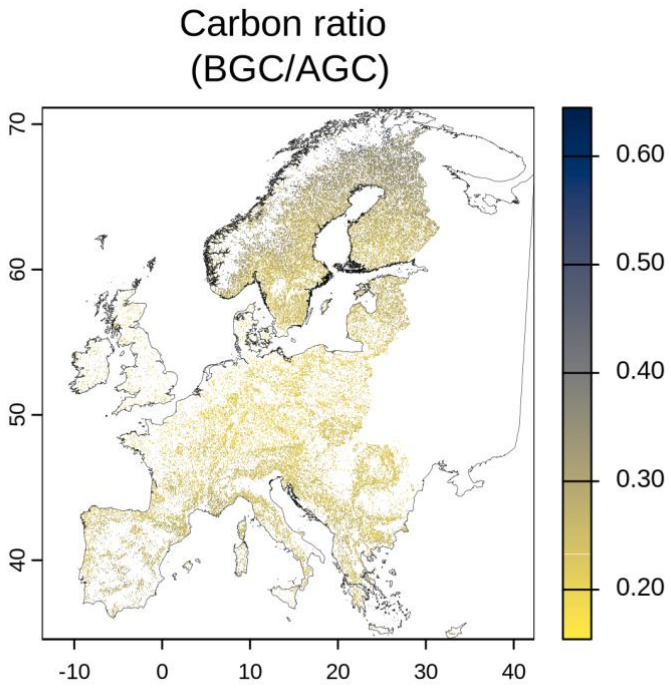

Figure 12 | Spatial distribution of carbon allocation between aboveground and belowground, equivalent to Root-to-Shoot ratio.

Validation of BGC map

Our BGC map broadly agrees with a mid-latitude peak of BGC, and higher carbon allocation in cool, moist, productive forests. We compared our belowground output to the Spawn et al., (2020)[2] BGC product. Across 1,000 points, our BGC had a correlation of (r^2=0.089, p<0.001), mean difference of -3.8 Mg C ha^{-1} and RMSE of 8. While some divergence is expected due to the resolution difference, the offsets likely capture forest composition changes and biomass accumulation over the ten-year interval. The lower offsets observed across Scandinavia may suggest higher model stability in large, contiguous forest blocks compared to the more heterogeneous forests of Central and Southern Europe. Rather than indicating model error, these offsets likely reflect the localized sensitivity of the higher resolution 10 m PathFinder products to contemporary forest structure changes that are smoothed in coarser, older datasets.

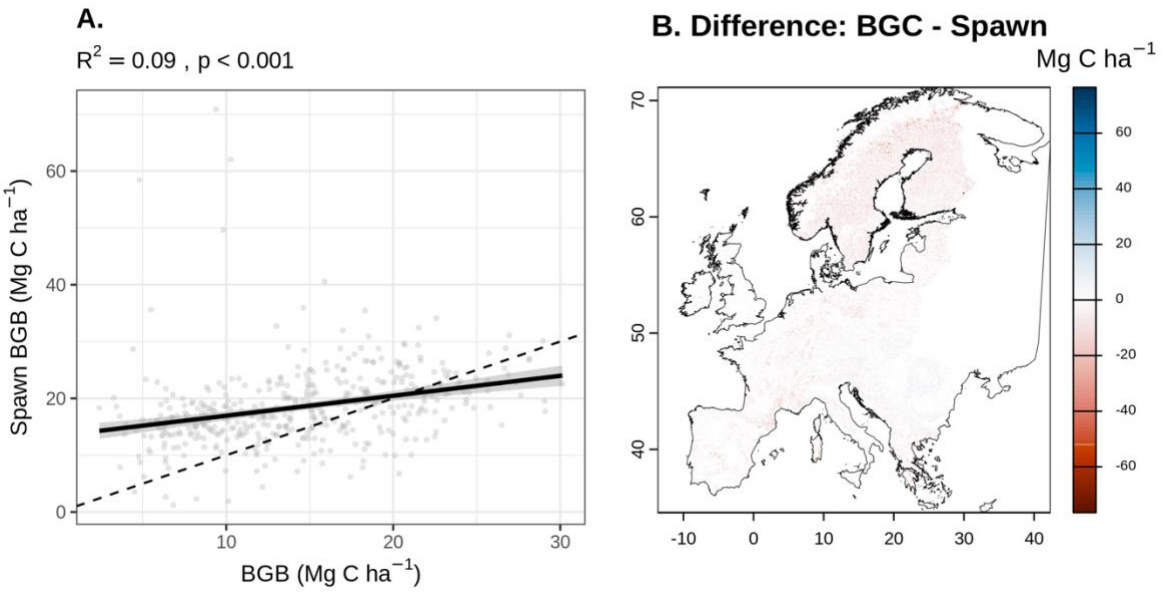

Figure 13 | Validation of BGC (calculated in this work) against Spawn et al., (2020)[2]. Carbon estimates extracted at 1000 points and compared (A: linear model r^2=0.09, p<0.001) and difference map of all forest pixels.

2.3 Soil organic carbon

Soil organic carbon was calculated using the HoliSoils gridded dataset[14]. We calculate SOC stock for the top 0-30 cm using a standard equation (e.g. Szatmári et al., (2024)[15]):

$$SOC_s = 0.1 \cdot SOC_c \cdot BD \cdot (1 - CF) \cdot Depth$$

Where:

SOC_s: soil organic carbon stock (Mg C ha^{-1})

SOC_c: soil organic carbon content (g kg^{-1})

BD: bulk density (g cm^{-3})

CF: coarse fragments (n, cm^3 cm^{-3})

$Depth$: depth of soil layer (cm)

[14] Calisto, L., Batjes, N. H., & van Oostrum, A. (2023). D3.4 Open access harmonised soil database. HoliSoils (EU Horizon 2020 Grant agreement ID: 101000289) (p. 1726). ISRIC - World Soil Information. https://doi.org/10.1152/ajplegacy.1975.229.6.1726

[15] Szatmári, G., Laborczi, A., Mészáros, J., Takács, K., Benő, A., Koós, S., Bakacsi, Z., & Pásztor, L. (2024). Gridded, temporally referenced spatial information on soil organic carbon for Hungary. Scientific Data, 11(1), 1312. https://doi.org/10.1038/s41597-024-04158-3

The HoliSoils[14] products provide gridded data on mean SOC content, bulk density and coarse fragments (divided by 100 to convert percentage to fraction) for the 0-30 cm layer (Figure 14 A-C). We use the above equation to generate SOC stock for the topsoil (Figure 14). The SOC stock was reprojected and aligned to the PathFinder[3] 100 m grid to ensure consistent integration.

Current data availability is restricted as HoliSoils[14] only provides data for the top 30 cm of the soil profile. In many European forests, particularly boreal forests and other forests on peatlands, substantial carbon is stored below 30 cm. Peat soils, deep organic horizons, and mountain regions with thick accumulations of organic matter are therefore underestimated in our SOC component. A global effort to map soil organic carbon[16] indicates that more than double the carbon is stored at depth (0-100 cm), compared to topsoil (0-30 cm), highlighting the importance of incorporating deeper soil data when available. A future refinement could incorporate deeper soil layers when they are available from HoliSoils[14]. Consequently, the SOC values reported here should be viewed as a conservative estimate of total soil carbon.

Additionally, the HoliSoils products are restricted to the EU CORINE 2018 forest classes, a more restricted spatial extent than PathFinder products. Consequently our SOC content, BD, CF and SOC stock lack data in 24% of biomass-defined forest pixels (Figure 16). For maximum transparency, we chose to avoid the high uncertainty associated with interpolating soil properties across such a large and heterogeneous spatial extent, restricting our efforts to the high-confidence spatial intersection of the biomass and soil products.

[16] Crézé, C., Saatchi, S., Kwon, N., Yang, Y., & Li, S. (2025). High-resolution global map (100 m) of soil organic carbon reveals critical ecosystems for carbon storage. ESSD – Land/Land cover and land use. https://doi.org/10.5194/essd-2025-294

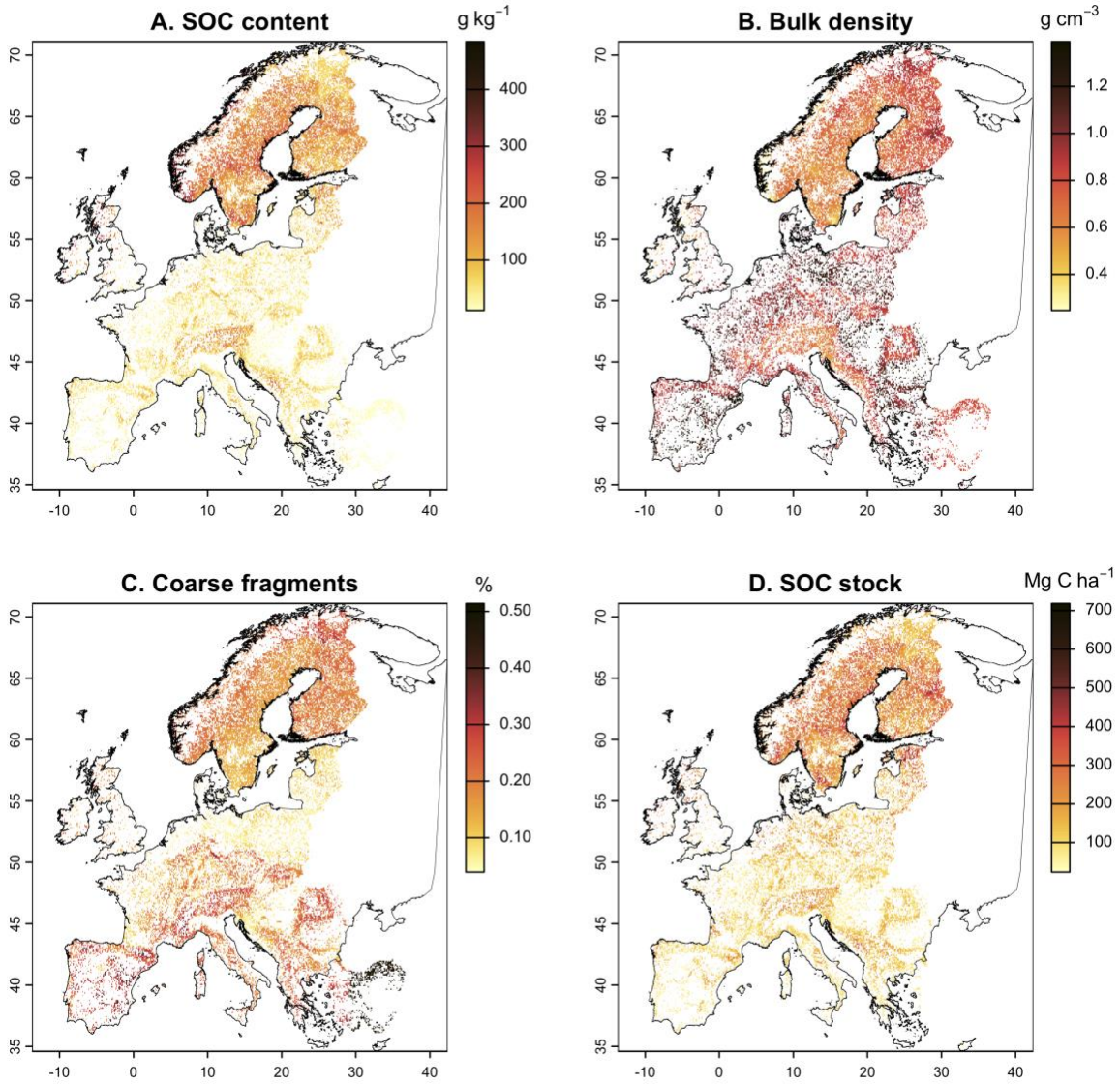

Figure 14 | Soil organic carbon content (A), bulk density (B), coarse fragments (C) and total soil organic carbon stock (SOC) in the top 0-30 cm[14].

Forests on peat

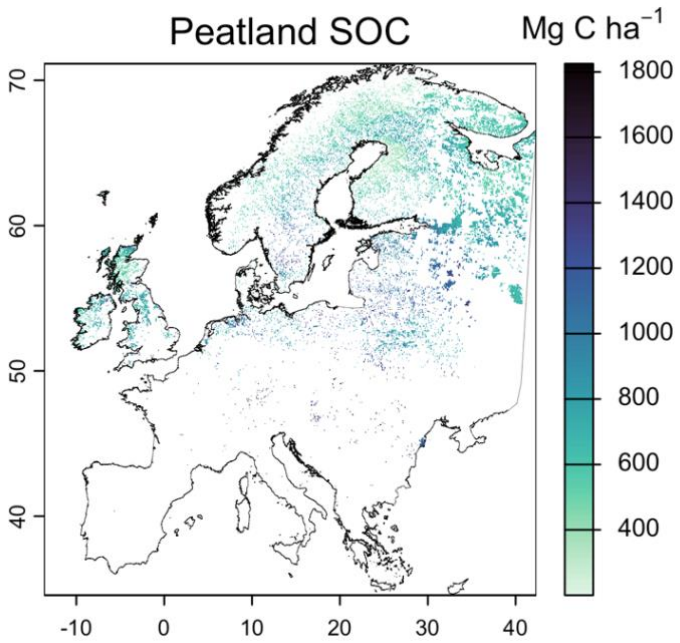

Figure 15 | Peat soil organic carbon (includes all land cover types)[18].

Peatlands make up only 7 % of forest pixels in the project area, but they contribute a disproportionately large share of total carbon stock due to their depth. We integrated the PEATGRIDS global dataset (1 x 1 km resolution)[17,18] (Figure 15) with our SOC map (Figure 14D). We removed any peat outliers >3IQR, ensured that both peat SOC and SOC stock in topsoil shared the same units and resolution. Using a conditional overlay, we prioritised peat pixels, while the remaining forest area with data was populated with the topsoil SOC estimate. Our approach ensures that carbon stocks in forests on peatlands are accurately represented alongside higher-resolution topsoil data for some of the wider project area. The inclusion of the peat data extends the SOC stock coverage in many boreal and bog forest

[17] Widyastuti, M. T., Minasny, B., Padarian, J., Maggi, F., Aitkenhead, M., Beucher, A., Connolly, J., Fiantis, D., Kidd, D., Ma, Y., Macfarlane, F., Robb, C., Rudiyanto, Setiawan, B. I., & Taufik, M. (2025). Digital mapping of peat thickness and carbon stock of global peatlands. *CATENA*, *258*, 109243. https://doi.org/10.1016/j.catena.2025.109243

[18] Widyastuti, M. T., Minasny, B., Padarian, J., & Maggi, F. (2024). PEATGRIDS: Mapping global peat thickness and carbon stock via digital soil mapping approach, dataset (2.0.1) [Data set]. Zenodo. https://doi.org/10.5281/zenodo.15070037

regions that were not covered by HoliSoils alone, although the final composite SOC map is spatially limited in that it lacks data for 24% of the forest pixels in the study.

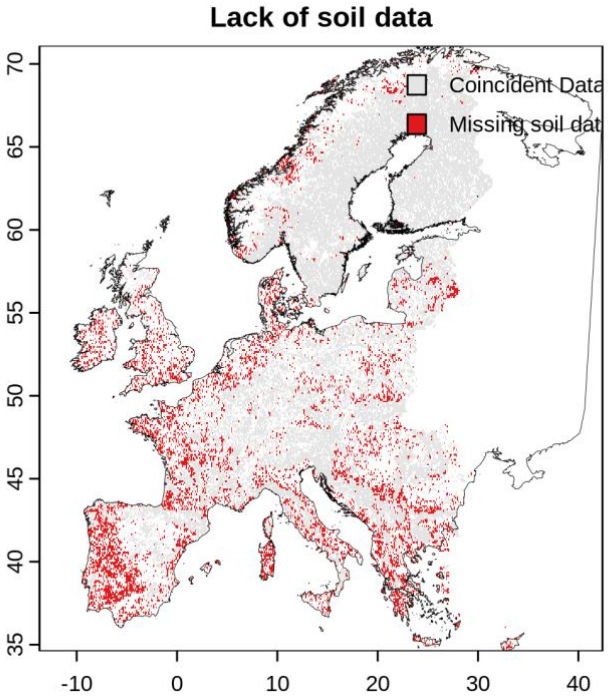

Figure 16 | Spatial disagreement between forest biomass and soil organic carbon (SOC) datasets. Grey pixels indicate where PathFinder forest biomass data and PEATGRIDS or HoliSoils SOC data are coincident. Red pixels are forest areas where soil data is unavailable (24% of the forest biomass pixels) and were not included in the SOC stock or total carbon maps.

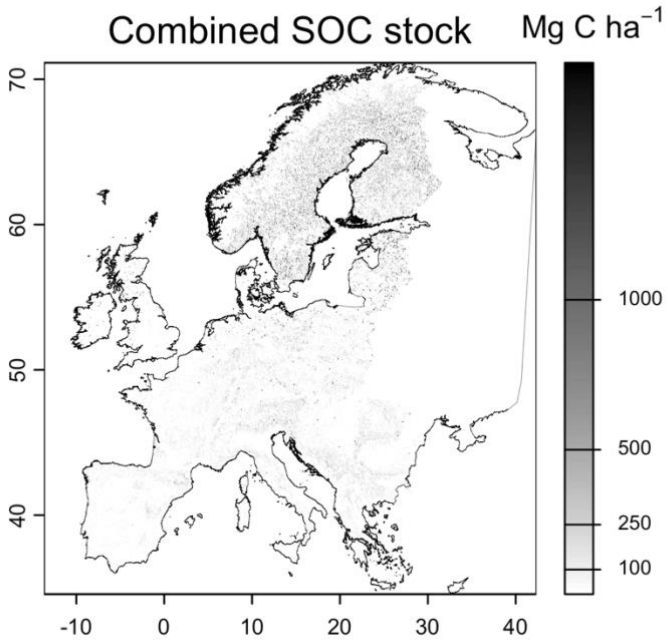

Figure 17 | Integrated soil organic carbon stock combining topsoil SOC (0-30 cm) (Figure 14) with deep-peat carbon estimates (Figure 15). Peatland pixels identified from PEATGRIDS[17] were assigned deep-peat carbon values, whereas non-peat forest pixels retain the 0-30 cm calculated SOC stock (0-30 cm).

The spatial pattern of SOC largely reflects what has been found in previous studies[19], although those studies included information for deeper soil layers. We find the highest SOC in the northwestern UK and Finland, where peatlands dominate. Lower SOC is found in mountainous regions, in the drier Mediterranean, and in regions which have been intensively cultivated.

2.4 Total carbon

Total forest carbon (Figure 18) was calculated per pixel by summing AGC, BGC and SOC. To display the relative carbon density of the input layers we include a standardised four panel

[19] Crézé, C., Saatchi, S., Kwon, N., Yang, Y., & Li, S. (2025). High-resolution global map (100 m) of soil organic carbon reveals critical ecosystems for carbon storage. ESSD – Land/Land cover and land use. https://doi.org/10.5194/essd-2025-294

figure (Figure 19) as well as mapping SOC, the dominant carbon pool, as a fraction of total carbon (Figure 20).

Across the project area, in 2020, forests in the region stored an estimated 37 Gt of carbon (AGC + BGC + SOC). This is 11 Gt of aboveground biomass carbon (AGC), 2 Gt of belowground biomass carbon (BGC), and 31 Gt of soil organic carbon (SOC). Soil carbon is the largest carbon pool, accounting for approximately 68% of total ecosystem carbon (Figure 20) in European forests.

Our estimates are very conservative. Particularly the SOC estimate which is constrained both vertically and horizontally. It focuses on peatland soil data plus the 0-30 cm topsoil layer, and is restricted to the spatial extent of the HoliSoils product. In choosing not to gap-fill the SOC stock we avoid introducing the uncertainties of large-scale interpolation. Despite our intentional underestimate of soil carbon stock, our results highlight the dominant contribution of soils and the importance of integrating above-, below-ground and soil pools in European carbon accounting.

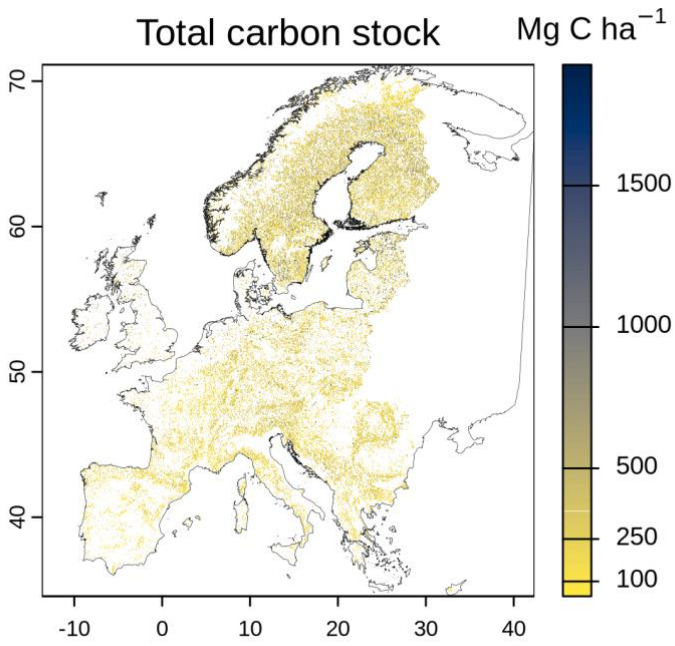

Figure 18 | Total carbon (AGC + BGC +SOC).

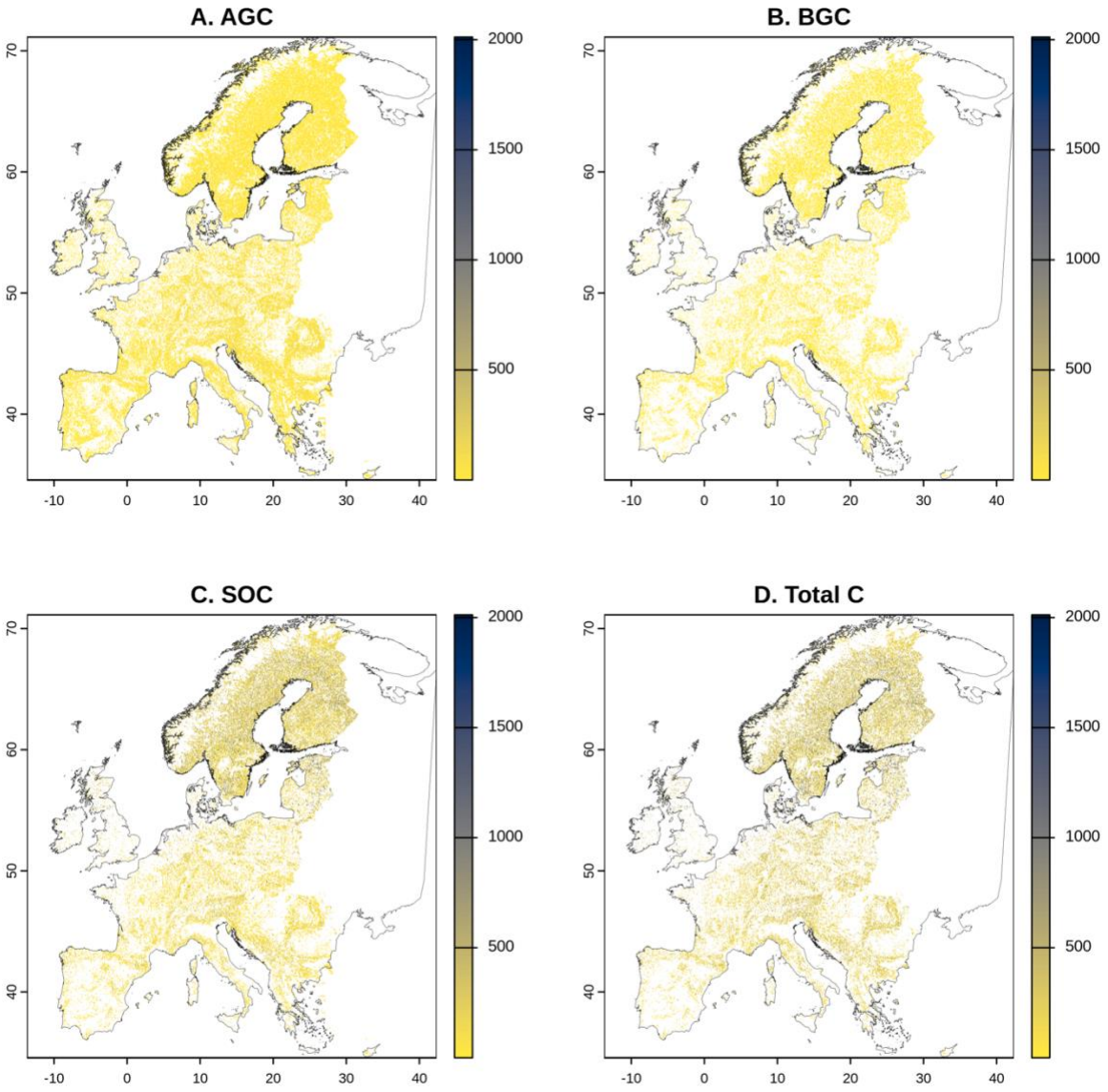

Figure 19 | Carbon pools and total carbon, displayed with standardised scale (Mg C ha^{-1}).

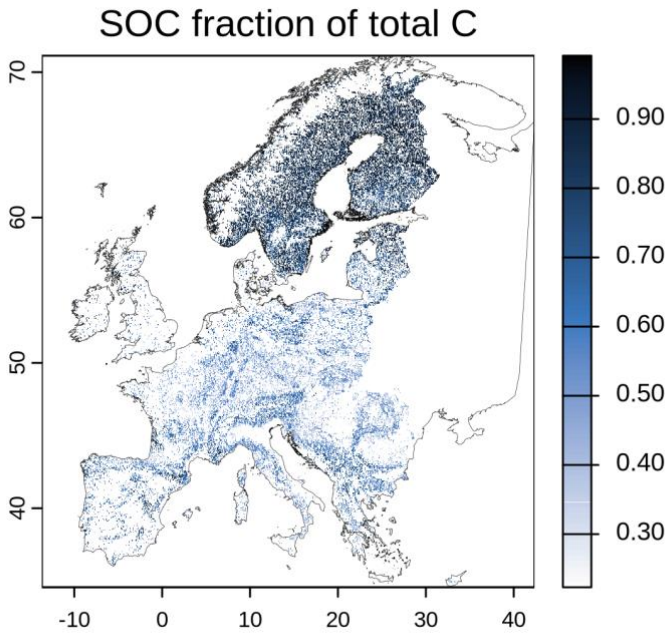

Figure 20 | Fraction of total carbon which is soil carbon.

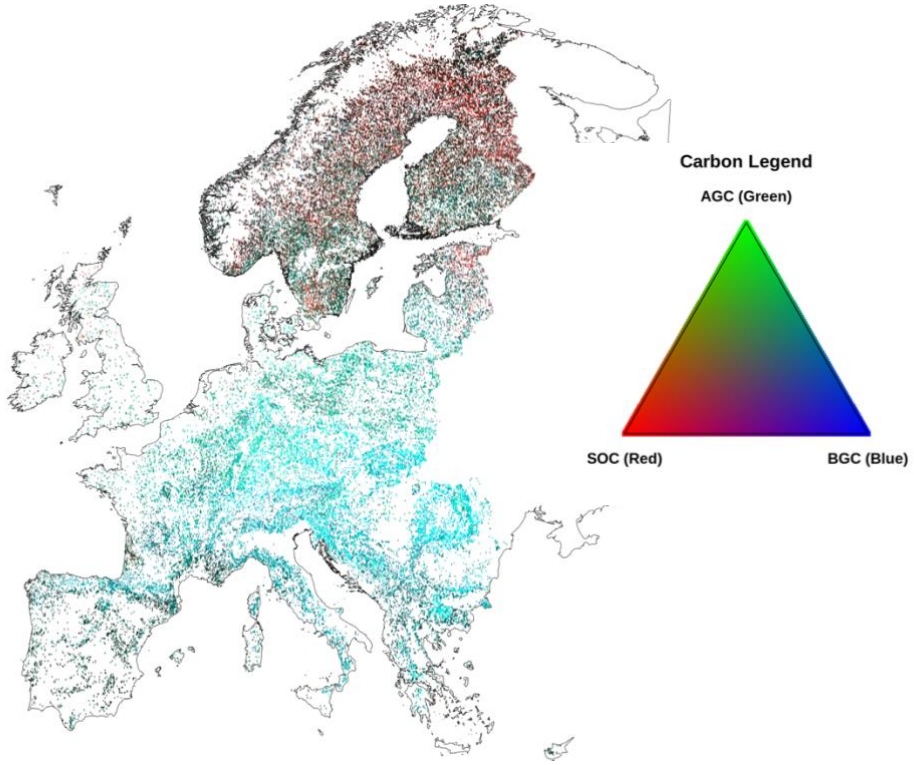

Figure 21 | European forest carbon composition 2020. RGB composite of SOC (red), AGC (green), and BGC (blue). Secondary colours indicate the dominance of multiple carbon pools: yellow (high SOC and AGC), cyan (high AGC and BGC), and magenta (high SOC and BGC). Transparency is modulated by total carbon stock highlighting areas of high forest carbon density.

3. Summary

We provide a high-resolution product for total carbon density of European forests. By combining NFI-aligned aboveground biomass estimates, climate- and phylogeny-specific carbon fractions, and harmonised soil datasets, the resulting 100 m carbon maps capture the major ecological gradients that shape carbon storage across European forests. In 2020, forests across the project area stored an estimated 37 Gt of carbon: 11 Gt in aboveground biomass, 2 Gt in belowground biomass and at least 31 Gt of soil organic carbon. Our analysis indicates that European forests store approximately 4.3% of the global total, as Pan et al., (2024)[20] estimated global forest carbon stock to be 870 ± 61 Pg C. Notably, soils represent the largest pool, approximately 84 % of total ecosystem carbon, and we lack data across forests and on soil carbon at depth for the majority of forest pixels, so this is an underestimate. The integrated dataset offers a robust baseline for 2020 and is intended to support subsequent identification of carbon-rich ecosystems in Europe and as model input data validations within SafeNet. This deliverable therefore provides a comprehensive foundation for understanding forest carbon dynamics, evaluating trade-offs, and informing forest conservation and management strategies across the region.

Table 4 | Summary of carbon stocks for forest pixels in project area.

		This study			State of Europe's forests[21]	
Carbon pool	Total C (Gt)	Mean (Mg ha^{-1})	Median (Mg ha^{-1})	% of total C	Mean (Mg ha^{-1})	%
AGC	11	42	33	30	51.2	29
BGC	2	14	13	6	12.8	7
SOC	31	196	153	84	-	54
Total	37	276	244	100	-	

[20] Pan, Y., Birdsey, R. A., Phillips, O. L., Houghton, R. A., Fang, J., Kauppi, P. E., Keith, H., Kurz, W. A., Ito, A., Lewis, S. L., Nabuurs, G.-J., Shvidenko, A., Hashimoto, S., Lerink, B., Schepaschenko, D., Castanho, A., & Murdiyarso, D. (2024). The enduring world forest carbon sink. *Nature*, *631*(8021), 563–569. https://doi.org/10.1038/s41586-024-07602-x

[21] FOREST EUROPE. (2020). State of Europe's forests. https://foresteurope.org/wp-content/uploads/2016/08/SoEF_2020.pdf

4. Associated data

Table 5 | Overview of input data.

Input	Item	Variables	Spatial resolution	Temporal reference	Geographic coverage	Source
AGB	PathFinder forest structure maps	AGB (Mg ha^{-1}) % AGB from conifers	10 m (aggregated to 100 m)	2020	Europe (excluding Russia)	Miettinen et al., 2025
Climate domain	Koppen-Geiger climate classification 1991-2020	Climate classification per pixel	~1 km	1991-2020	Global	Beck et al., 2023
Forest domain	PathFinder forest structure maps	Proportion of AGB from conifers	30 m (aggregated to 100 m)	2020	Europe (excluding Russia)	Miettinen et al., 2025
Regenerative origin	JRC global map of forest types 2020, v1	Natural forest locations	10 m	2020	Global	Bourgoin et al., 2026
Soil components	HoliSoils soil property dataset	SOC content (g kg^{-1}) BD (g cm^{-3}) CF (%)	100 m		Europe (excluding Russia)	Calisto et al., 2023
Peat	PEATGRIDS	Carbon stock (Mg ha^{-1})	1 km		Global	Widyastuti et al., 2025

Table 6 | Methods, equations, coefficients or conversion factors used in this analysis.

Item	Source
Wood carbon fraction	Martin et al., 2018
AGC to BGC	Reich et al., 2014, Spawn et al., 2020
SOC	Szatmári et al., 2024, Widyastuti et al., 2025

Table 7 | List of raster outputs, forest carbon density map layers available on Zenodo.

Item
Aboveground carbon (Mg C ha^{-1})
Belowground carbon (Mg C ha^{-1})
Soil organic carbon (Mg C ha^{-1})
Total carbon (Mg C ha^{-1})

SafeNet

Safeguarding Biodiversity and Carbon-rich Forest **Net**works in Europe

Project Coordination

Jukka Forsman | jukka.forsman@luke.fi

Mikko Peltoniemi | mikko.peltoniemi@luke.fi

Jacqueline Moustakas-Verho | jacqueline.moustakas-verho@luke.fi

Project Communications

Mathilde Vidal | mathilde@erinn.eu

More Information

Website | safenet-project.eu

Bluesky | @safenet-eu.bsky.social

LinkedIn | @SafeNet Project

Funded by the European Union

Funded by the European Union under the Horizon Europe Programme, Grant Agreement No. 101181981 (SafeNet). Views and opinions expressed are, however, those of the author(s) only and do not necessarily reflect those of the European Union or European Research Executive Agency (REA). Neither the European Union nor the granting authority can be held responsible for them.